12-28-2011

Gravity Wave Heating and Cooling of the Thermosphere: Sensible Heat Flux and Viscous Flux of Kinetic Energy

Michael P. Hickey Ph.D.
Embry-Riddle Aeronautical University, hicke0b5@erau.edu

R. L. Walterscheid
The Aerospace Corporation

G. Schubert
Institute of Geophysics and Planetary Physics, University of California

Scholarly Commons Citation

Hickey, M. P., R. L. Walterscheid, and G. Schubert (2011), Gravity wave heating and cooling of the thermosphere: Sensible heat flux and viscous flux of kinetic energy, J. Geophys. Res., 116, A12326, doi: https://doi.org/10.1029/2011JA016792

Gravity wave heating and cooling of the thermosphere: Sensible heat flux and viscous flux of kinetic energy

M. P. Hickey,[1] R. L. Walterscheid,[2] and G. Schubert[2,3]

Received 28 April 2011; revised 26 October 2011; accepted 27 October 2011; published 28 December 2011.

[1] Total wave heating is the sum of the convergence of the sensible heat flux and the divergence of the viscous flux of wave kinetic energy. Numerical simulations, using a full-wave model of the viscous damping of atmospheric gravity waves propagating in a nonisothermal atmosphere, are carried out to explore the relative contributions of these sources of wave heating as a function of wave properties and altitude. It is shown that the sensible heat flux always dominates in the lower thermosphere, giving a lower region of heating and an upper stronger region of cooling. The heating due to the divergence of the viscous flux of kinetic energy is significant only for fast waves (horizontal phase speed greater than about 120 m s^{-1}). The faster the wave is, the greater the heating in the upper thermosphere can be. The viscous heat source in per unit mass terms can greatly exceed the sensible heat source for fast waves and might be a significant heat source for the middle and upper thermosphere.

Citation: Hickey, M. P., R. L. Walterscheid, and G. Schubert (2011), Gravity wave heating and cooling of the thermosphere: Sensible heat flux and viscous flux of kinetic energy, *J. Geophys. Res.*, *116*, A12326, doi:10.1029/2011JA016792.

1. Introduction

[2] Early investigations recognized that the energy carried by atmospheric gravity waves must ultimately be deposited in the background thermosphere when the waves dissipate due to molecular viscosity [*Pitteway and Hines*, 1963; *Hines*, 1965]. Subsequent numerical simulations suggested that dissipating gravity waves might heat the thermosphere by several tens of kelvins per day [*Klostermeyer*, 1973]. It was also understood that while molecular thermal conductivity dissipates gravity waves and increases the entropy of the atmosphere, it does not lead to heating of the thermosphere [*Klostermeyer*, 1973].

[3] *Walterscheid* [1981] reexamined the effect of dissipating gravity waves by considering the sensible heat flux in the second-order expansion of the energy equation. It was found that a dissipating gravity wave drives a downward sensible heat flux or enthalpy flux. The divergence of the sensible heat flux is positive at high altitudes, cooling the background gas. At lower altitudes the divergence of the sensible heat flux is negative, equivalent to an accumulation of sensible heat and concomitant heating of the background atmosphere. Thus, the wave removes energy from higher altitudes and deposits it at lower altitudes. Due to the decrease of mean density with increasing altitude, the cooling rate J/ρ (where J is the heating rate per unit volume and ρ is the mass density) at high altitude is far greater than the heating rate at lower altitude.

[4] Subsequent numerical simulations further demonstrated the significance of the sensible heat flux divergence. For example, while *Young et al.* [1997] inferred from Galileo Probe observations that dissipating gravity waves might heat the thermosphere of Jupiter, more complete simulations by *Matcheva and Strobel* [1999] and *Hickey et al.* [2000] showed that the sensible heat flux divergence driven by dissipating gravity waves mainly cools Jupiter's upper atmosphere. Other simulations using the full-wave model have shown that the same result holds for gravity waves dissipating in the atmospheres of Earth [*Walterscheid and Hickey*, 2005] and Mars [*Parish et al.*, 2009]. Measurements of sensible heat flux and its divergence by *Gardner and Liu* [2007] based on lidar observations of winds and temperatures in the 85–100 km altitude range of Earth's atmosphere show that the sensible heat flux is downward in this altitude range consistent with dissipating gravity waves.

[5] Our full-wave model simulations of irreversible wave effects on the atmosphere are based on including all terms in the second-order expansion of the energy equation. The relevant terms for the thermosphere are the second-order viscous term, the divergence of the viscous flux of kinetic energy, the second-order sensible heat flux convergence term, the term describing the work done by pressure gradients on the gas, and a term describing the work done against buoyancy by the second-order Eulerian mean velocity [*Schubert et al.*, 2003, 2005]. (See also discussions of wave heating effects in the work of *Schoeberl et al.*

[1]Department of Physical Sciences, Embry-Riddle Aeronautical University, Daytona Beach, Florida, USA.
[2]Space Science Applications Laboratory, Aerospace Corporation, El Segundo, California, USA.
[3]Department of Earth and Space Sciences, University of California, Los Angeles, California, USA.

0148-0227/11/2011JA016792

[1983], *Medvedev and Klaassen* [2003], *Becker* [2003, 2004], *Yiğit et al.* [2008], and *Yiğit and Medvedev* [2009].)

[6] An interesting observation noted from our previous full-wave modeling studies is that to a very good approximation for typical waves the heating and cooling due to the sensible heat flux convergence equals the total heating/cooling due to the contribution of all four terms in the second-order energy equation [*Hickey et al.*, 2000]. In other words, the total heating or cooling is given primarily by the sensible heat flux convergence. This equivalence has also been noted by *Gavrilov and Shved* [1975] and *Akmaev* [2007].

[7] The near equality of sensible heat flux convergence and total heating rate does not, in fact, hold at all altitudes for all waves and so we explore the conditions under which the equivalence is valid. In general, total wave heating may be written as the sum of the heating due to the convergence and divergence, respectively, of the sensible heat flux and viscous flux of wave kinetic energy [*Schubert et al.*, 2003]. We present numerical solutions showing regions of the atmosphere in which the two sources of wave warming and cooling dominate. We find that the viscous flux of wave kinetic energy can create a second region of wave heating at higher altitudes for certain waves.

2. Theory

[8] *Schubert et al.* [2003] have shown that (their equation (3))

$$\bar{\rho}c_p Q_{tot} = \langle \underline{\nabla}\cdot\left(\underline{v}'\cdot\underline{\underline{\sigma}}'_m\right)\rangle - \frac{d}{dz}\left(\bar{\rho}c_p\langle w'T'\rangle\right), \tag{1}$$

where Q_{tot} is the total heating/cooling rate (degrees per unit time) for dissipating gravity waves, c_p is the specific heat at constant pressure, $\bar{\rho}$ is the mean density of the atmosphere, z is the vertical coordinate, v' is the wave induced velocity, $\underline{\underline{\sigma}}'_m$ is the wave induced viscous stress tensor, w' is the wave vertical velocity, T' is the wave induced temperature perturbation, and angular brackets denote a horizontal average.

[9] Equation (1) states that the total heating/cooling rate (energy per unit time per unit volume) for dissipating gravity waves is given by the negative vertical divergence (convergence) of the sensible heat flux (denoted by $\bar{\rho}c_p Q_{SH}$, where Q_{SH} has units of degrees per unit time) plus the divergence of the energy flux associated with viscous stresses acting on the boundary of a fluid element. To be consistent with the usual practice of referring to pressure working on a fluid element as the wave energy flux, we refer to the working by viscous stresses as the viscous flux of wave kinetic energy [*Landau and Lifshitz*, 1987]. The divergence of this flux is hereinafter denoted $\bar{\rho}c_p\underline{\nabla}\cdot\underline{F}_{\rm vis}$ (the factor $\bar{\rho}c_p$ allows $\underline{\nabla}\cdot\underline{F}_{\rm vis}$ to have units of degrees per unit time). Accordingly, we can write

$$\bar{\rho}c_p Q_{SH} = -\frac{d}{dz}\left\{\bar{\rho}c_p\langle w'T'\rangle\right\}, \tag{2}$$

$$\bar{\rho}c_p\underline{\nabla}\cdot\underline{F}_{\rm vis} = \left\langle\underline{\nabla}\cdot\left(\underline{\underline{\sigma}}'_m\cdot\underline{v}'\right)\right\rangle, \tag{3}$$

$$Q_{\rm tot} = Q_{SH} + \underline{\nabla}\cdot\underline{F}_{\rm vis}. \tag{4}$$

For waves for which $\partial/\partial z \gg \partial/\partial x_i$ and x_i is any horizontal coordinate (1) may be written approximately as

$$\bar{\rho}c_p Q_{\rm tot} = -\frac{d}{dz}\left[c_p\bar{\rho}\langle w'T'\rangle - \mu_m d\left\langle\frac{1}{2}u'^2\right\rangle/dz\right], \tag{5}$$

where μ_m is the coefficient of dynamic viscosity and u' is the magnitude of the horizontal wind fluctuation.

[10] We show next that for typical waves the sensible heat flux term dominates the viscous flux term in the lower thermosphere. The sensible heat flux for typical gravity waves is given approximately as

$$c_p\bar{\rho}\langle w'T'\rangle = -H\frac{\hat{m}^2\hat{\nu}_m}{\kappa}A, \tag{6}$$

where $\kappa = R/c_p$, R is the gas constant and H is the scale height of the background atmosphere [*Walterscheid*, 1981]. Carets refer to scaled quantities defined by $\hat{m} = Hm$ and $\hat{\nu}_m = \eta/H^2$, where $\hat{m}$ is nondimensional, m is the dimensional vertical wave number, $\hat{\nu}_m$ has the units of frequency, and η is the vertical diffusivity of momentum. The quantity $A = \bar{\rho}(g^2/N^2)\langle(T'/\bar{T})^2\rangle$ is the horizontally averaged wave available potential energy [*Lighthill*, 1978; *Walterscheid and Schubert*, 1990], g is the acceleration of gravity, and N is the Brunt-Väisälä frequency. For weakly damped waves the strongest height dependence is through η ($\eta \propto \exp(z/H)$) with the result

$$\frac{d}{dz}\left(c_p\bar{\rho} < w'T' >\right) \approx -\frac{\hat{m}^2\hat{\nu}_m}{\kappa}A. \tag{7}$$

[11] The divergence of the viscous flux of kinetic energy is given by

$$\frac{d}{dz}\mu_m d\left(\bar{\rho}^{-1}K\right)/dz \approx \hat{\nu}_m K, \tag{8}$$

where $K = \bar{\rho}u'^2$. Except for waves very near evanescence $\hat{m}^2/\kappa \gg 1$. Assuming an approximate equipartition of energy between available potential energy and kinetic energy gives the result that the heating due to the sensible heat flux far exceeds the heating due to the viscous flux of kinetic energy (equipartition breaks down for frequencies near the Coriolis frequency).

[12] Dominance of $\underline{\nabla}\cdot\underline{F}_{\rm vis}$ over Q_{SH} is favored for waves that can propagate high in the thermosphere. For such waves $\hat{m}^2/\kappa$ in (7) is not necessarily large and in addition for strongly attenuating waves $d(\bar{\rho}^{-1}K)/dz$ in (8) becomes large.

[13] In order to propagate to great heights a wave must escape strong attenuation at lower altitudes due to evanescence and viscous dissipation. A wave's ability to do this is governed by its phase speed and wave frequency. It is seen by an examination of the approximate (anelastic) dispersion relation (valid for most gravity waves)

$$m^2 = \frac{1}{c^2}\left(N^2 - \omega^2\right) - \frac{1}{4H^2}, \tag{9}$$

that waves that can propagate to great heights are those that can maintain values of m^2 that are positive in the lower

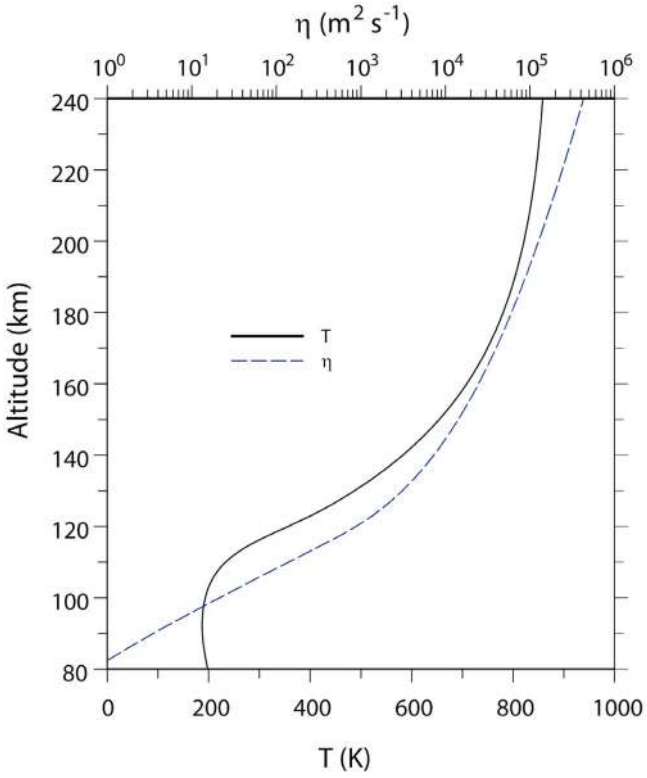

Figure 1. Plot of the mean temperature (solid curve) and kinematic viscosity (dashed curve) versus altitude.

thermosphere (to avoid attention due to evanescence) and are not too large (to avoid viscous attenuation). Here c is the horizontal phase speed. Waves with low phase speeds must have frequencies close to the Brunt-Vaisala frequency to avoid viscous absorption. These waves are sensitive to small differences between N and ω and it seems unlikely that there is a choice of frequency that gives suitable values of m^2 over a sufficiently large range of altitudes where temperature varies with height. For large phase speeds, however, the requirement that N be close to ω is relaxed and it is far easier to satisfy the conditions on m^2 allowing propagation to great heights.

[14] In section 3 we perform numerical simulations of gravity wave dissipation and explicitly compare the two terms on the right side of (1). The numerical solutions allow us to determine the altitude range for which the heating may be dominated by either Q_{SH} or $\underline{\nabla}\cdot\underline{F}_{\rm vis}$.

3. Numerical Calculations

[15] Simulations are performed using our full-wave model that describes the propagation of linear, steady acoustic-gravity waves through a windy, rotating, nonisothermal mean state atmosphere including ion drag, the eddy diffusion of heat and momentum and molecular dissipation due to viscosity and thermal conductivity [*Hickey et al.*, 1997; *Walterscheid and Hickey*, 2001; *Schubert et al.*, 2003]. The lower boundary is the ground, and the upper boundary is placed high in the thermosphere (700 km for these simulations) where a sponge layer prevents reflected waves from traveling very far. The MSIS model [*Hedin*, 1991] for northern summer, midlatitude, night, and average solar and geomagnetic activity is used to specify the mean state using the same input values used by *Walterscheid and Hickey* [2011]. Figure 1 shows the altitude variation of the mean atmospheric temperature (solid curve) and the kinematic viscosity (dashed curve). The temperature exhibits a minimum value of ~187 K near 93 km altitude (the mesopause), and then increases at greater altitudes. At 240 km altitude its value is 859 K, and it asymptotes to a value of 877 K in the upper thermosphere (not shown). The kinematic viscosity increases from a value of 1 $m^2\ s^{-1}$ at 80 km altitude to greater than $4 \times 10^5\ m^2\ s^{-1}$ at 240 km altitude. By 500 km altitude (not shown) it has increased to $\sim 10^8\ m^2\ s^{-1}$.

[16] We perform simulations for several different waves. Mean winds, eddy diffusion, and ion drag are not considered. Without loss of generality, propagation is assumed to be eastward in all cases. Wave speeds c = 60, 120, 180, and 240 m s^{-1} and wave frequencies of some fraction of a reference value ω_0 giving waves on the verge of evanescence in the lower thermosphere are considered. We chose wave periods as follows: we require that the full adiabatic dispersion relation [*Einaudi and Hines*, 1970] for the vertical wave number squared (m^2) equals zero for each value of c at 175 km altitude in the lower thermosphere. We perform simulations for values of ω given by $\omega = \omega_0/\alpha$, where α = 1.2, 2.4 and 4.8, and where ω_0 is the value of ω for which m^2 is zero. These values of ω along with the associated value of horizontal wave number k are given in Table 1. This range of values gives waves that vary from waves that attain evanescence in the lower thermosphere to waves that are internal throughout the thermosphere (neglecting viscous effects). Wave amplitudes were chosen to give a value of wave amplitude defined as the magnitude of $T'/\bar{T}$ of 5% at the amplitude maximum. This is on the high side of typical amplitudes, but is far below the limiting value given by wave breakdown [*Walterscheid and Schubert*, 1990]. The altitudes of the amplitude maxima for the various waves are shown in Table 2. The heating is a quadratic function of wave amplitude and the change in heating for different assumed wave amplitudes must be scaled accordingly.

4. Results

[17] Figure 2 shows the values of m^2 versus altitude for c = 60 m s^{-1} for the various values of α. For α = 1.2 the wave

Table 1. Period and Horizontal Wavelength for Each Combination of Phase Speed and the Parameter α[a]

c (m/s)	α = 1.2	α = 2.4	α = 4.8
60	11.92 min, 42.90 km	23.83 min, 85.80 km	47.66 min, 171.59 km
120	10.87 min, 78.28 km	21.74 min, 156.56 km	43.49 min, 313.11 km
180	9.92 min, 107.18 km	19.85 min, 214.36 km	39.70 min, 428.72 km
240	9.02 min, 129.95 km	18.05 min, 259.89 km	36.10 min, 519.78 km

[a]For more information, see text.

Table 2. Altitude of the Maximum in the Wave Amplitude Defined as the Magnitude of $T'/\bar{T}$

c (m/s)	α = 1.2	α = 2.4	α = 4.8
60	123.0 km	120.8 km	118.5 km
120	183.7 km	154.5 km	136.5 km
180	188.3 km	200.3 km	171.8 km
240	171.0 km	252.8 km	208.1 km

approaches evanescence in the upper part of the lower thermosphere. For α = 2.4 and 4.8 the values of m^2 are similar to each other and the corresponding waves are well within the internal regime at all altitudes shown.

[18] Figure 3 shows the heating due to Q_{SH} and $\underline{\nabla}\cdot\underline{F}_{\rm vis}$ and the total heating $Q_{\rm tot}$ versus altitude for all values of α. The total heating shown here and all subsequent such figures is calculated using (1). All waves are viscously damped in the lower thermosphere where the heating due to the viscous flux of kinetic energy is small so the total heating is essentially the heating due to the sensible heat flux. The structure seen just below 125 km is a manifestation of partial wave trapping related to the steep gradients near the peaks in the m^2 curves seen in Figure 2. The peak warming for the α = 1.2 wave is ~45 K d^{-1} near 130 km, while the peak cooling is ~100 K d^{-1} near 170 km. Solutions for α = 2.4 and 4.8 show that the altitudes of peak heating and cooling occur progressively lower as α increases and the peak values of warming and cooling diminish. For α = 4.8 the peak cooling occurs near 140 km altitude and the peak warming near 115 km, with peak values of ~−15 K d^{-1} for the cooling and ~10 K d^{-1} for the warming. The diminished warming and cooling occurring at lower altitudes for α = 2.4 and 4.8 is a result of increased viscous damping at lower altitudes due to smaller vertical wavelengths.

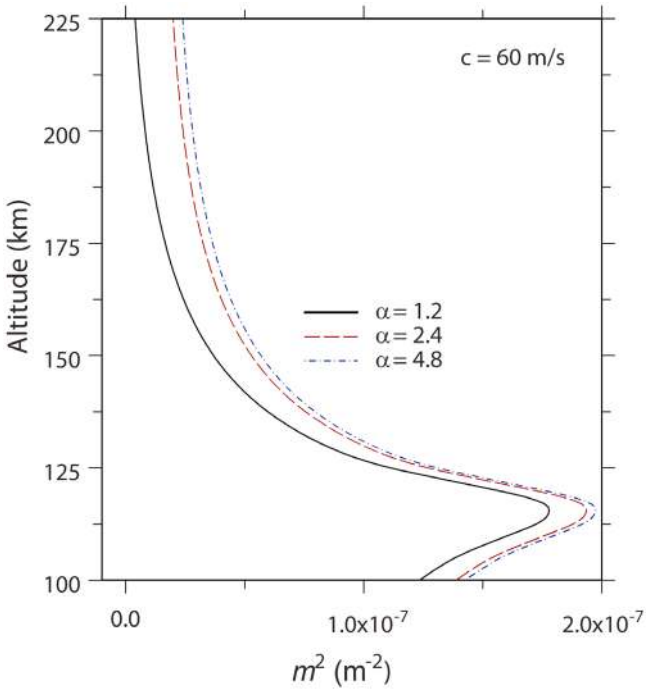

Figure 2. Plot of the vertical wave number squared m^2 versus altitude for a wave with phase speed 60 m s^{-1} for three values of wave period: 11.9 min (α = 1.2), 23.8 min (α = 2.4) and 47.7 min (α = 4.8).

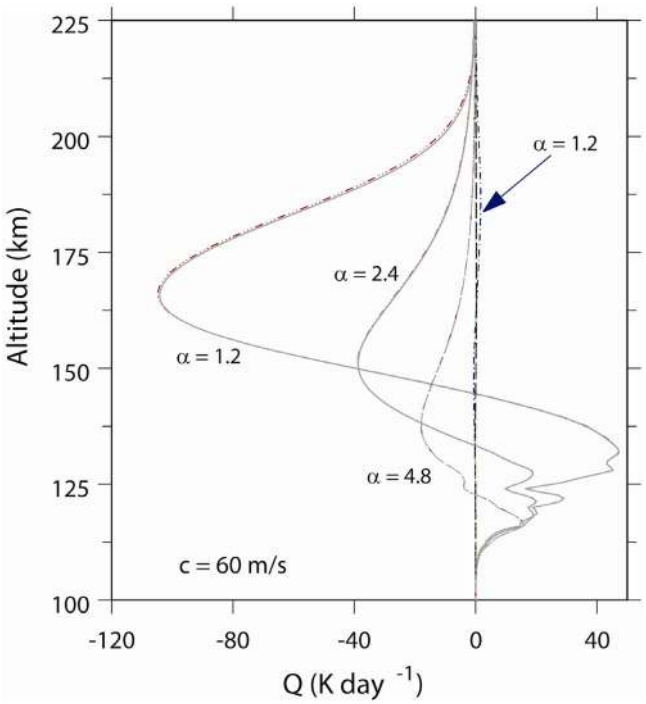

Figure 3. Plots of wave heating per unit mass for the same waves as in Figure 2, Total wave heating (solid), convergence of the sensible heat flux (dash triple dot) and divergence of the viscous flux of kinetic energy (dash dot).

[19] Figure 4 shows the values of m^2 versus altitude for c = 120 m s^{-1} and various values of α. For α = 1.2, the wave attains evanescence near 220 km and is weakly evanescent above this altitude. For α = 2.4 and 4.8 the waves are internal at all altitudes but have significantly larger wavelengths than for c = 60 m s^{-1}. Figure 5 shows the corresponding values of heating. As for c = 60 m s^{-1} the dominant contribution to the total heating by far is Q_{SH}, although the contribution due to $\underline{\nabla}\cdot\underline{F}_{\rm vis}$ is clearly discernable for α = 1.2. Compared to c = 60 m s^{-1} the peak cooling and warming are found at higher altitudes and have larger peak values. For α = 1.2 the warming and cooling peaks are located near 160 km and 220 km, respectively, with peak values of ~−325 K d^{-1} and 225 K d^{-1}. We note that the wave-induced heat flux does not depend on whether the wave is evanescent or internal and even though the wave is evanescent at altitudes above ~220 km significant cooling occurs at higher altitudes [*Walterscheid*, 1981]. Results for α = 2.4 and 4.8 indicate diminishing contributions from $\underline{\nabla}\cdot\underline{F}_{\rm vis}$ relative to Q_{SH}, as well as diminishing total warming and cooling and a decrease in the altitudes of the peak warming and cooling.

[20] Figure 6 shows m^2 versus altitude in the lower thermosphere for c = 180 m s^{-1} for various values of α. For α = 1.2 the wave attains evanescence near 190 km altitude. For α = 2.4 and 4.8 the waves are internal, but are significantly closer to evanescence than for c = 120 m s^{-1}.

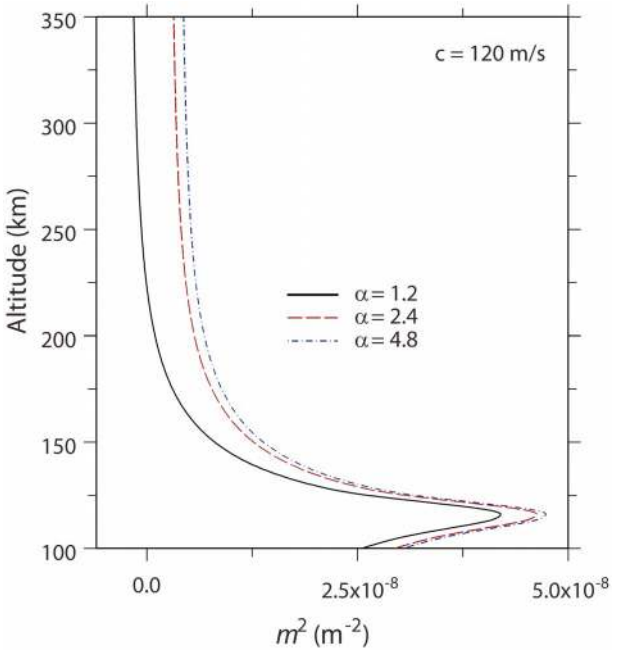

Figure 4. Same as Figure 2 except for phase speed of 120 m s^{-1} and periods: 10.9 min (α = 1.2), 21.7 min (α = 2.4) and 43.5 min (α = 4.8).

[21] Figure 7 shows the heating and cooling as a function of altitude for α = 1.2. The results are similar to those for c = 120 m s^{-1}, with the exception that the contribution from $\underline{\nabla}\cdot\underline{F}_{vis}$, though still minor at all altitudes is larger and is discernable even at fairly low altitudes. Compared to 120 m s^{-1} the peak heating and cooling are reduced by nearly a factor of 2 and the peaks are found about 25 km higher.

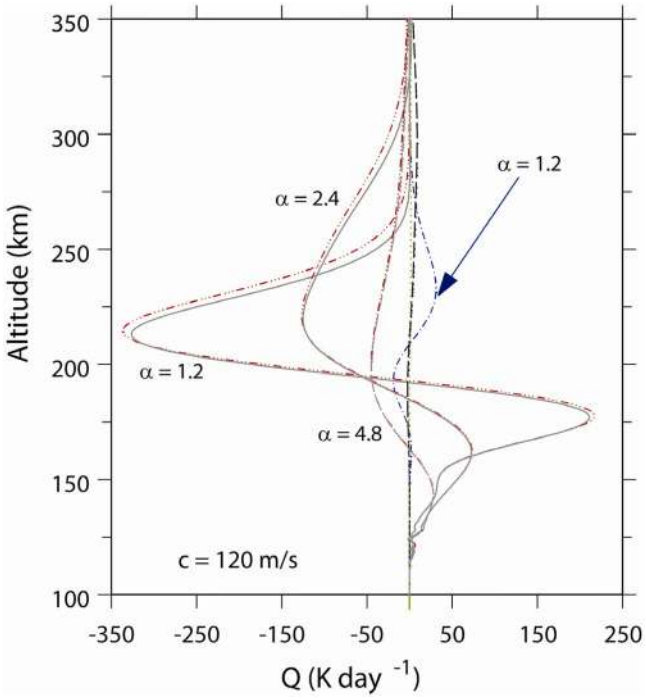

Figure 5. Same as Figure 3 except for waves in Figure 4.

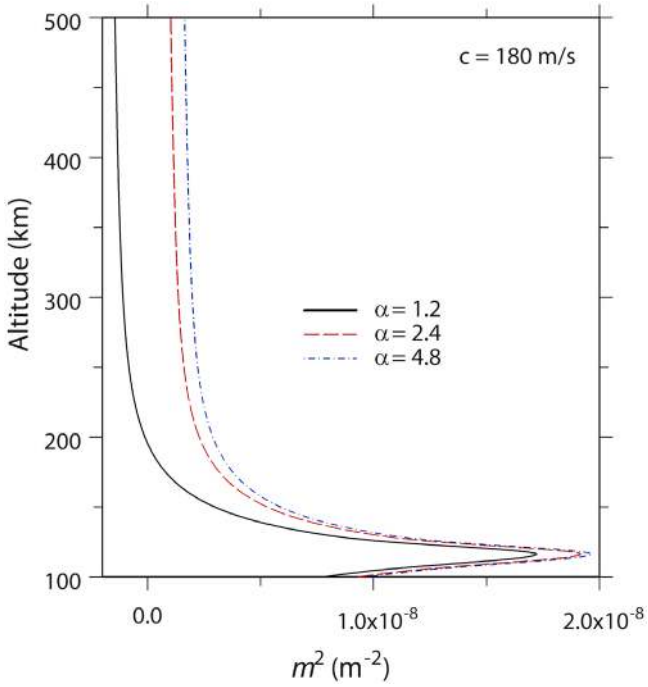

Figure 6. Same as Figure 2 except for phase speed of 180 m s^{-1} and periods: 9.9 min (α = 1.2), 19.9 min (α = 2.4) and 39.7 min (α = 4.8).

[22] Figure 8 shows the heating and cooling for c = 180 m s^{-1} for α = 2.4. For this value of α, the wave avoids evanescence and because of the small positive values of m^2 it is not strongly damped until it attains

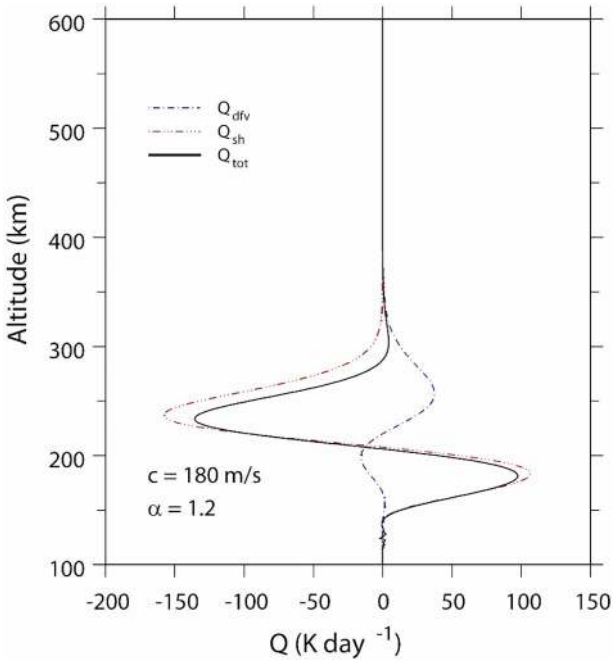

Figure 7. Plot of wave heating per unit mass for the α = 1.2 wave in Figure 6, total wave heating (solid), convergence of the sensible heat flux (dash triple dot) and divergence of the viscous flux of kinetic energy (dash dot).

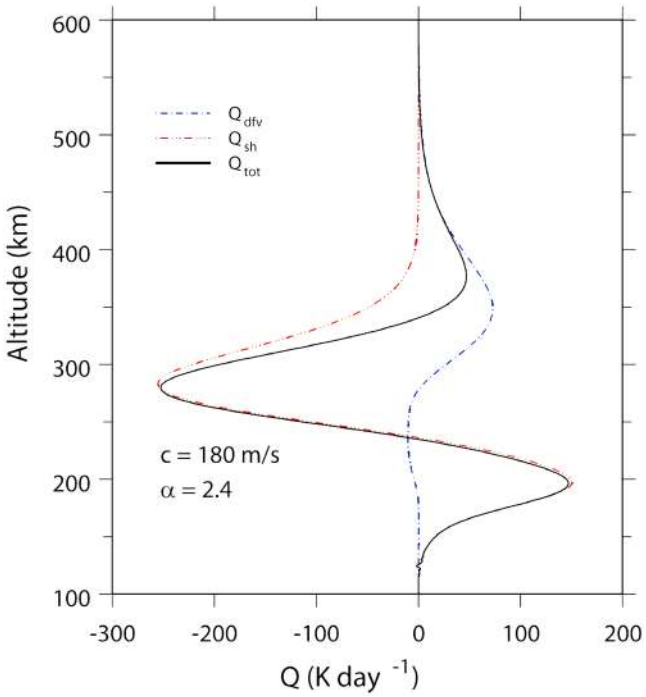

Figure 8. Same as Figure 7 except for the $\alpha = 2.4$ wave in Figure 6.

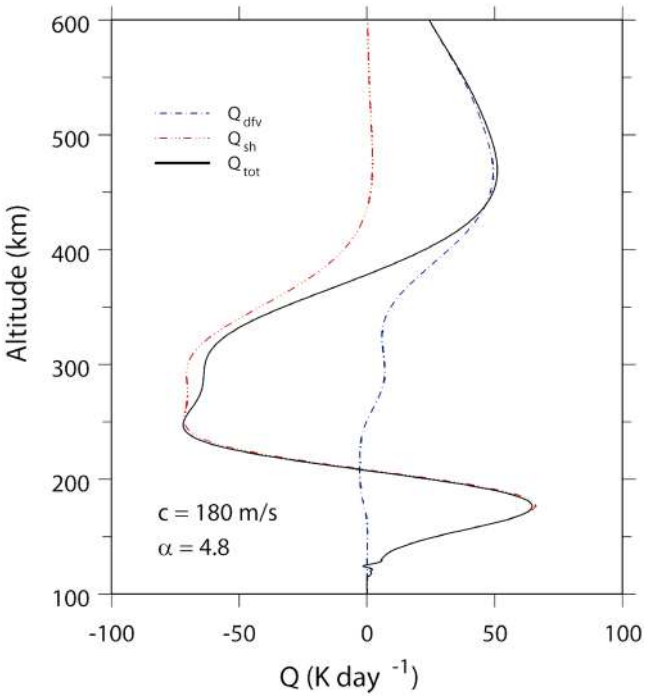

Figure 9. Same as Figure 7 except for the $\alpha = 4.8$ wave in Figure 6.

altitudes above ~200 km. The regions of warming and cooling due to the sensible heat flux are shifted upward by ~25 km, while the peak values remain roughly the same. The most significant difference is the occurrence of a higher region of net warming peaking near 380 km. This warming is due to the dominance of the heating due to the divergence of the viscous flux of kinetic energy. The net heating is comparatively modest with peak heating of ~50 K d^{-1} compared to the lower-level warming of ~150 K d^{-1}. The results for $\alpha = 4.8$ (Figure 9) are similar except that the heating and cooling due to the sensible heat flux are diminished by about a factor of two in the region of heating and a factor of three in the region of cooling, and the latter region is considerably broader. The upper region of heating peaks near 450 km and the heating is similar in magnitude to that of the lower region and occurs over a much thicker region. The diminishment of Q_{SH} is consistent with an increased rate of scale-dependent viscous dissipation at lower thermospheric altitudes.

[23] Figure 10 shows the values of m^2 versus altitude in the lower thermosphere for $c = 240$ m s^{-1} for various values of α. For $\alpha = 1.2$ the wave attains evanescence near 180 km altitude and is strongly evanescent above ~200 km. For $\alpha = 2.4$ and 4.8 the waves are internal, but are close to evanescence at all altitudes above about 200 km.

[24] Figure 11 shows the heating and cooling as a function of altitude for $\alpha = 1.2$. The results are similar to those for $c = 180$ m s^{-1} except the peak warming and cooling are diminished by about a factor of three and the contribution to Q_{tot} by $\underline{\nabla}\cdot\underline{F}_{\text{vis}}$ is greater. Figure 12 shows the heating and cooling for $\alpha = 2.4$. Compared to the results for $c = 180$ m s^{-1} regions of heating and cooling dominated by Q_{SH} peak somewhat higher and have much greater peak values, consistent with reduced viscous absorption. The most notable difference is the much stronger heating in the region where Q_{tot} is dominated by $\underline{\nabla}\cdot\underline{F}_{\text{vis}}$, the peak value

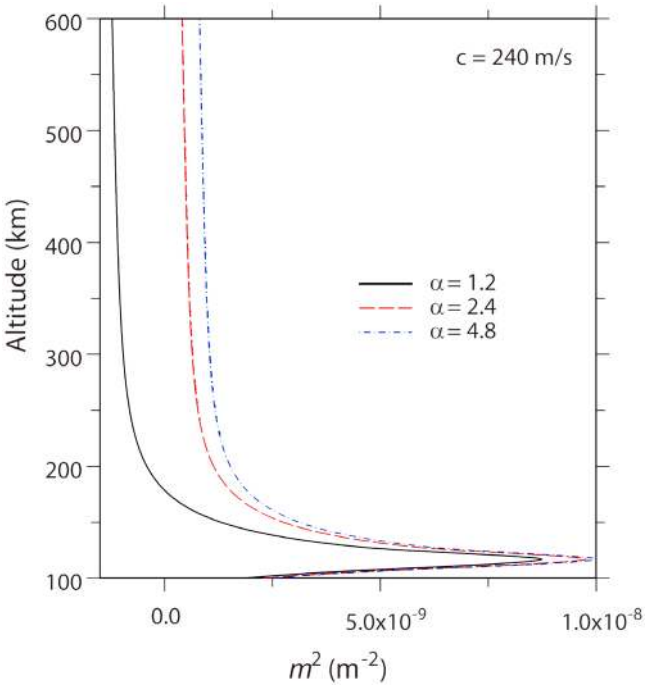

Figure 10. Same as Figure 2 except for phase speed of 240 m s^{-1} and periods: 9.0 min ($\alpha = 1.2$), 18.1 min ($\alpha = 2.4$) and 36.1 min ($\alpha = 4.8$).

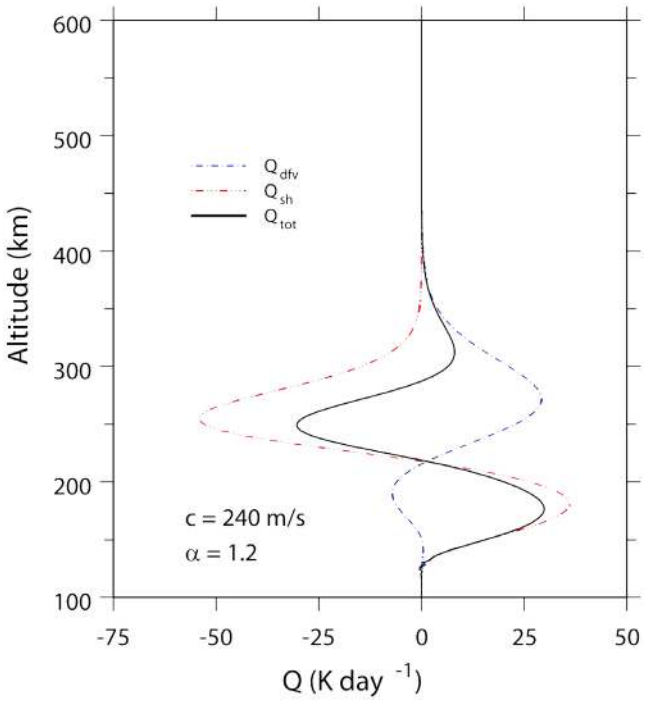

Figure 11. Plots of wave heating per unit mass for the α = 1.2 wave in Figure 10, total wave heating (solid), convergence of the sensible heat flux (dash triple dot) and divergence of the viscous flux of kinetic energy ((dash dot).

being ~2/3 of the peak value in the lower region of heating.

[25] Figure 13 shows the heating and cooling as a function of altitude for α = 4.8. The upper region of heating is displaced upward and peaks near 550 km. The peak warming in this region now far exceeds the peak heating in the lower region, being about 3 times greater. Peak values attain nearly 250 K d^{-1}. The heating Q_{SH} remains the strongly dominant source of wave heating in the lower thermosphere.

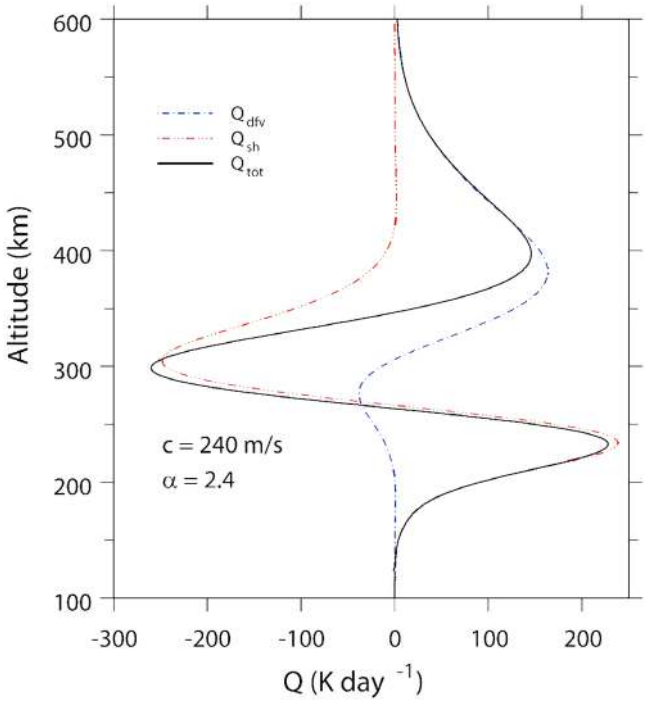

Figure 12. Same as Figure 11 except for the α = 2.4 wave in Figure 10.

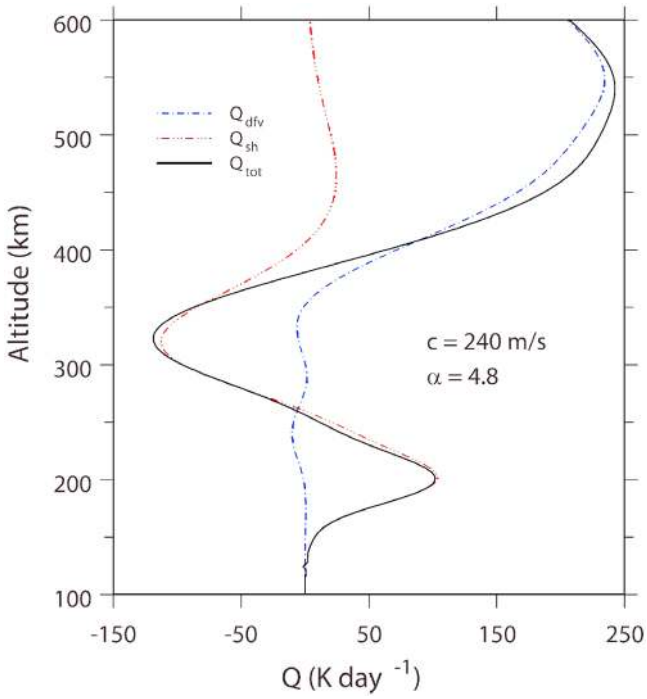

Figure 13. Same as Figure 11 except for the α = 4.8 wave in Figure 10.

[26] At altitudes where the effect of the divergence of the viscous flux exceeds that of the sensible heat flux the wave amplitude and energy flux can be quite small. Figure 14 shows the relative temperature perturbation amplitude and the vertical component of the horizontal averaged energy flux for c = 240 m s^{-1} and for α = 1.2. Of all the waves examined here this one has the largest high altitude heating rates associated with the divergence of the viscous flux. Here the vertical component of the horizontal-time averaged energy flux, $\langle F_z \rangle$, is given by

$$\langle F_z \rangle = \langle p'w' \rangle - \frac{\mu_m}{2}\left\langle \frac{d}{dz}\left(|u'|^2 + |w'|^2\right)\right\rangle - \frac{\kappa_m}{2\bar{T}}\left\langle \frac{d}{dz}|T'|^2 \right\rangle.$$

Here all symbols are as previously defined, and κ_m is the coefficient of molecular thermal conductivity. The wave amplitude (solid curve in Figure 14) peak of ~5% occurs just above 200 km altitude, after which it decreases with increasing altitude, reaching ~0.2% at 600 km altitude. The energy flux (dashed-triple-dotted curve in Figure 14) remains approximately constant with a value of ~3 × 10^{-5} W m^{-2} at the lowest altitudes shown, but then begins to decrease noticeably above ~150 km altitude as the kinematic viscosity increases. It continues to decrease

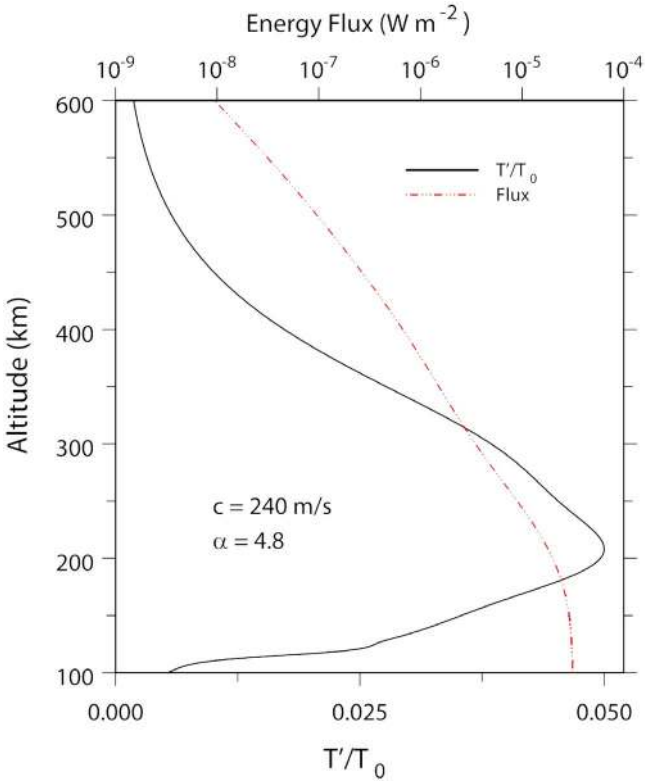

Figure 14. Plot of the relative temperature perturbation amplitude (solid curve) and the vertical component of the energy flux (dashed curve) for the wave in Figure 13.

as altitude increases, reaching a value of $\sim 10^{-8}$ W m^{-2} at 600 km altitude.

5. Discussion and Conclusions

[27] Total wave heating is the sum of the convergence of the sensible heat flux and the divergence of the viscous flux of wave energy. For most waves $Q_{\rm tot} \approx Q_{SH}$, but $Q_{\rm tot} = Q_{SH} + \underline{\nabla}\cdot\underline{F}_{\rm vis}$, and the conditions under which the term $\underline{\nabla}\cdot\underline{F}_{\rm vis}$ may be important and even dominant have not been previously explored. We have shown that Q_{SH} should dominate $\underline{\nabla}\cdot\underline{F}_{\rm vis}$ for molecular dissipation that is not too strong. We have demonstrated, using a numerical full-wave model, that the total wave heating and cooling rate $Q_{\rm tot}$ is almost entirely provided by the sensible heat flux convergence Q_{SH} for internal gravity waves that dissipate in the lower thermosphere. These tend to be rather slow waves. For fast waves that reach altitudes in the middle and upper thermosphere with significant amplitude the divergence of the viscous flux of kinetic energy $\underline{\nabla}\cdot\underline{F}_{\rm vis}$ can dominate. In the lower thermosphere Q_{SH} is dominant for all waves considered.

[28] The heating due to the viscous flux of kinetic energy may be quite significant. The fast waves have maximum amplitudes $T'/\bar{T}$ = 5% occurring between about 190 and 250 km. Such waves can grow from waves that have very small amplitudes at lower altitudes ($\ll$1% at 90 km). Since slower waves are filtered by evanescence before they can reach high thermospheric altitudes it seems likely that the spectrum in the middle thermosphere is dominated by fast waves. Values of $T'/\bar{T}$ consistent with our assumed peak amplitude are seen in the middle thermosphere [*Ford et al.*, 2006; *Innis and Conde*, 2002]. The heating rates we calculate suggest that wave heating due to the viscous flux of kinetic energy might be a significant contributor to the heat budget of the middle thermosphere [*Banks and Kockarts*, 1973].

[29] While the sensible heat flux for dissipating gravity waves is downward [*Walterscheid*, 1981], our results (not shown) show that the viscous flux of wave kinetic energy is upward. Hence, while the sensible heat flux leads to cooling at high altitudes where heat is extracted and warming at low altitudes where it is deposited, the reverse is true for the viscous flux. In the case of the sensible heat flux the magnitude of the cooling effect exceeds the heating effect because the energy is taken from a region of low density and deposited in a region of high density. In the viscous flux case the magnitude of the heating effect far exceeds the cooling effect because the energy is taken from a region of higher density and deposited in a region of lower density.

[30] **Acknowledgments.** MPH was supported by the National Science Foundation under grants ATM-0408407 and ATM-0639293. RLW was supported by NASA Grant NNX08AM13G and by NSF Grant ATM 0737557. GS acknowledges support from the NASA Mars Fundamental Research program under grant NNG05GM06G.

[31] Robert Lysak thanks the reviewers for their assistance in evaluating this paper.

References

Akmaev, R. A. (2007), On the energetics of mean-flow interactions with thermally dissipating gravity waves, *J. Geophys. Res.*, *112*, D11125, doi:10.1029/2006JD007908.

Banks, P. M., and G. Kockarts (1973), *Aeronomy, Part B*, 355 pp., Academic, San Diego, Calif.

Becker, E. (2003), Frictional heating in global climate models, *Mon. Weather Rev.*, *131*, 508–520, doi:10.1175/1520-0493(2003)131<0508:FHIGCM>2.0.CO;2.

Becker, E. (2004), Direct heating rates associated with gravity wave saturation, *J. Atmos. Sol. Terr. Phys.*, *66*, 683–696, doi:10.1016/j.jastp.2004.01.019.

Einaudi, F., and C. O. Hines (1970), WKB approximation in application to acoustic-gravity waves, *Can. J. Phys.*, *48*, 1458–1471, doi:10.1139/p70-185.

Ford, E. A. K., A. L. Aruliah, E. M. Griffin, and I. McWhirter (2006), Thermospheric gravity waves in Fabry-Perot Interferometer measurements of the 630.0 nm OI line, *Ann. Geophys.*, *24*, 555–566, doi:10.5194/angeo-24-555-2006.

Gardner, C. S., and A. Z. Liu (2007), Seasonal variations of the vertical fluxes of heat and horizontal momentum in the mesopause region at Starfire Optical Range, New Mexico, *J. Geophys. Res.*, *112*, D09113, doi:10.1029/2005JD006179.

Gavrilov, N. M., and G. M. Shved (1975), On the closure of equation system for the turbulized layer of the upper atmosphere, *Ann. Geophys.*, *31*, 375–387.

Hedin, A. E. (1991), Extension of the MSIS thermospheric model into the middle and lower atmosphere, *J. Geophys. Res.*, *96*, 1159–1172, doi:10.1029/90JA02125.

Hickey, M. P., R. L. Walterscheid, M. J. Taylor, W. Ward, G. Schubert, Q. Zhou, F. Garcia, M. C. Kelley, and G. G. Shepherd (1997), Numerical simulations of gravity waves imaged over Arecibo during the 10-day January 1993 campaign, *J. Geophys. Res.*, *102*, 11,475–11,489.

Hickey, M. P., R. L. Walterscheid, and G. Schubert (2000), Gravity wave heating and cooling in Jupiter's thermosphere, *Icarus*, *148*, 266–281, doi:10.1006/icar.2000.6472.

Hines, C. O. (1965), Dynamical heating of the upper atmosphere, *J. Geophys. Res.*, *70*, 177–183, doi:10.1029/JZ070i001p00177.

Innis, J. L., and M. Conde (2002), Characterization of acoustic–gravity waves in the upper thermosphere using Dynamics Explorer 2 Wind and Temperature Spectrometer (WATS) and Neutral Atmosphere Composition Spectrometer (NACS) data, *J. Geophys. Res.*, *107*(A12), 1418, doi:10.1029/2002JA009370.

Klostermeyer, J. (1973), Thermospheric heating by atmospheric gravity waves, *J. Atmos. Terr. Phys.*, *35*, 2267–2275, doi:10.1016/0021-9169(73)90142-6.

Landau, L. D., and E. M. Lifshitz (1987), *Fluid Mechanics*, 2nd ed., 539 pp., Pergamon, Oxford, U. K.

Lighthill, J. (1978), *Waves in Fluids*, 504 pp., Cambridge Univ. Press, New York.

Matcheva, K. I., and D. F. Strobel (1999), Heating of Jupiter's thermosphere by dissipation of gravity waves due to molecular viscosity and heat conduction, *Icarus*, *140*, 328–340, doi:10.1006/icar.1999.6151.

Medvedev, A. S., and G. P. Klaassen (2003), Thermal effects of saturating gravity waves in the atmosphere, *J. Geophys. Res.*, *108*(D2), 4040, doi:10.1029/2002JD002504.

Parish, H., G. Schubert, M. P. Hickey, and R. L. Walterscheid (2009), Propagation of tropospheric gravity waves into the upper atmosphere of Mars, *Icarus*, *203*, 28–37, doi:10.1016/j.icarus.2009.04.031.

Pitteway, M. L. V., and C. O. Hines (1963), The viscous damping of atmospheric gravity waves, *Can. J. Phys.*, *41*, 1935–1948, doi:10.1139/p63-194.

Schoeberl, M. R., D. F. Strobel, and J. P. Apruzese (1983), A numerical model of gravity wave breaking and stress in the mesosphere, *J. Geophys. Res.*, *88*, 5249–5259, doi:10.1029/JC088iC09p05249.

Schubert, G., M. P. Hickey, and R. L. Walterscheid (2003), Heating of Jupiter's thermosphere by the dissipation of upward propagating acoustic waves, *Icarus*, *163*(2), 398–413, doi:10.1016/S0019-1035(03)00078-2.

Schubert, G., M. P. Hickey, and R. L. Walterscheid (2005), Physical processes in acoustic wave heating of the thermosphere, *J. Geophys. Res.*, *110*, D07106, doi:10.1029/2004JD005488.

Walterscheid, R. L. (1981), Dynamical cooling induced by dissipating internal gravity waves, *Geophys. Res. Lett.*, *8*(12), 1235–1238, doi:10.1029/GL008i012p01235.

Walterscheid, R. L., and M. P. Hickey (2001), One-gas models with height-dependent mean molecular weight: Effects on gravity wave propagation, *J. Geophys. Res.*, *106*, 28,831–28,839.

Walterscheid, R. L., and M. P. Hickey (2005), Acoustic waves generated by gusty flow over hilly terrain, *J. Geophys. Res.*, *110*, A10307, doi:10.1029/2005JA011166.

Walterscheid, R. L., and M. P. Hickey (2011), Group velocity and energy flux in the thermosphere: Limits on the validity of group velocity in a viscous atmosphere, *J. Geophys. Res.*, *116*, D12101, doi:10.1029/2010JD014987.

Walterscheid, R. L., and G. Schubert (1990), Nonlinear evolution of an upward propagating gravity wave: Overturning, convection, transience and turbulence, *J. Atmos. Sci.*, *47*, 101–125, doi:10.1175/1520-0469(1990)047<0101:NEOAUP>2.0.CO;2.

Yiğit, E., and A. S. Medvedev (2009), Heating and cooling of the thermosphere by internal gravity waves, *Geophys. Res. Lett.*, *36*, L14807, doi:10.1029/2009GL038507.

Yiğit, E., A. D. Aylward, and A. S. Medvedev (2008), Parameterization of the effects of vertically propagating gravity waves for thermosphere general circulation models: Sensitivity study, *J. Geophys. Res.*, *113*, D19106, doi:10.1029/2008JD010135.

Young, L. A., R. V. Yelle, R. Young, A. Seiff, and D. B. Kirk (1997), Gravity waves in Jupiter's thermosphere, *Science*, *276*, 108–111, doi:10.1126/science.276.5309.108.

M. P. Hickey, Department of Physical Sciences, Embry-Riddle Aeronautical University, 600 S. Clyde Morris Blvd., Daytona Beach, FL 32114, USA. (michael.hickey@erau.edu)

G. Schubert, Department of Earth and Space Sciences, University of California, 595 E. Charles E. Young Dr., Los Angeles, CA 90095-1567, USA. (schubert@ucla.edu)

R. L. Walterscheid, Space Science Applications Laboratory, Aerospace Corporation, MS 260, 2350 E. El Segundo Blvd., El Segundo, CA 90245-4691, USA. (richard.walterscheid@aero.org)